Influence of a Medium on Capacitive Power Transfer Capability

Accepted for publication. DOI: 10.1109/WPW54272.2022.9853947

Cédric Lecluyse
Department of Electrical Engineering (ESAT)
KU Leuven, ELECTA Ghent
Ghent, Belgium
cedric.lecluyse@kuleuven.be

Ben Minnaert
Department of Electromechanics, Cosys-Lab
University of Antwerp
Antwerp, Belgium
ben.minnaert@uantwerpen.be

Simon Ravyts
Department of Electrical Engineering (ESAT)
KU Leuven, ELECTA Ghent
Ghent, Belgium
simon.ravyts@kuleuven.be

Michael Kleemann
Department of Electrical Engineering (ESAT)
KU Leuven, ELECTA Ghent
Ghent, Belgium
michael.kleemann@kuleuven.be

***Abstract*— Despite the advantages of capacitive power transfer (CPT), inductive power transfer (IPT) is still preferred. The reason: IPT systems have a gap power density in air that is 400 times greater. Conclusively, IPT can transmit more power than CPT over greater distances in air, but what about other media? This paper gives an answer on how media, different from air, influence the power transfer over different distances. First, we analyze theoretically the capacitive coupling with different media in the gap. Next, we simulate the CPT system using finite-element software and compared it with the theoretical analysis. Finally, we employ the results of the finite-element simulation in a power electronic simulation to examine the influence of the medium on the electrical power transfer.**

***Keywords*— wireless power transmission, capacitive power transmission, capacitive coupling, electric coupling, electric fields.**

I. Introduction

Wireless power transfer (WPT) is an emerging technology that enables more convenient, standardised and safer systems [1]. The most common WPT technology is inductive power transfer (IPT). This technology is based on energy transfer with magnetic fields. It employs coils at the primary and secondary side. Another WPT technology is capacitive power transfer (CPT). Here, energy is transferred via electric fields between metal plates at primary and secondary side [1]. Compared to IPT, CPT has the advantages of being cost effective, it does not bear transmission losses in the vicinity of metal objects and emits fewer EM disturbances [1]–[3].

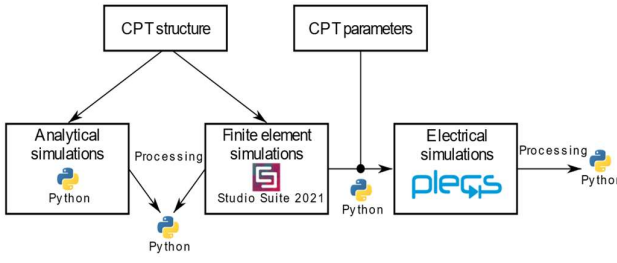

Fig. 1: Implemented methodology.

An important performance criterion of WPT is gap power density. The gap power density of IPT is 400 times greater than CPT with air as a medium [4]. This results in IPT being able to transmit higher powers over longer distances. For this reason, IPT is generally preferred over CPT for energy transfer through air. However, considering other solid or liquid media in the gap can be in favour of CPT technology. Also, CPT can become feasible in applications where IPT is limited by core materials [4].

This paper will investigate the research question: How do media different from air influence the power transfer of a CPT system over different distances? The methodology to investigate this question is shown in Fig. 1. The simulations are carried out by two commercial software programs. A Python script controls them allowing for an automated assessment. This script is responsible for both passing on the parameters and processing the results. The operation of the Python script and its interaction with the analytical, finite element and electrical simulations is shown in the flow chart in Fig. 2.

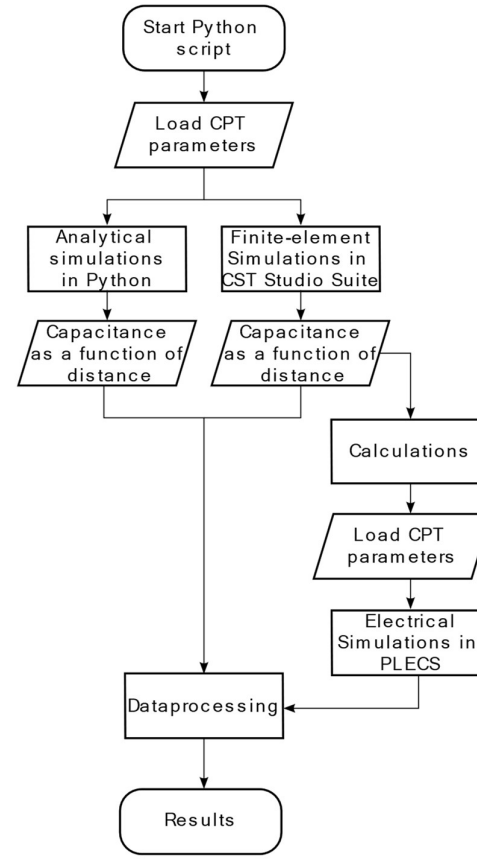

Fig. 2: Flowchart Python script.

First, the CPT structures will be analytically analysed in order to localise the capacitances present in the system. A Python script will determine the theoretical capacitance of the CPT coupling structure over different distances.

Second, a CPT structure model will be implemented in finite-element software CST Studio to yield more detailed results and to validate the theoretical findings. This will be done by using a Python script which reads the results from CST Studio Suite and compares them with previous

theoretical results. The previous theoretical calculation of the capacitances allows for the validation of the capacitance values obtained by finite-element analysis.

Third, a power electronic model of the CPT system will be set up in PLECS. A Python script will configure this model with the previously obtained capacitances, the input voltage, frequency, etc. in the power electronics model taking into account the limitations of present semiconductor switches. Then, the script will start the simulations and process the results. The simulation will yield the influence of the different media on the electrical power that can be transferred.

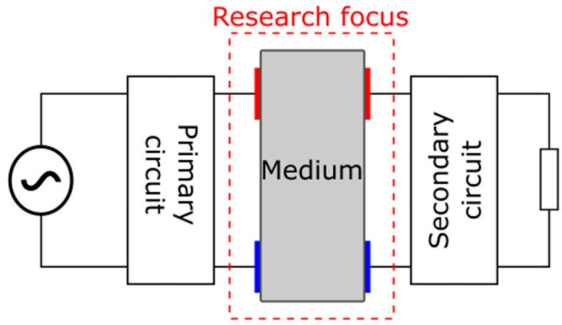

Fig. 3: Basic CPT structure.

II. Capacitive Coupling

A CPT system is commonly composed of two parallel pairs of metal plates with a medium between them, as shown in Fig. 3. A more detailed schematic equivalent circuit representation of this so-called four-plate structure is given in Fig. 4. The system consists of a pair of main coupling capacitors (C_{13} & C_{24}), two leakage capacitors (C_{12} & C_{34}) and two cross-coupling capacitors (C_{14} & C_{23}).

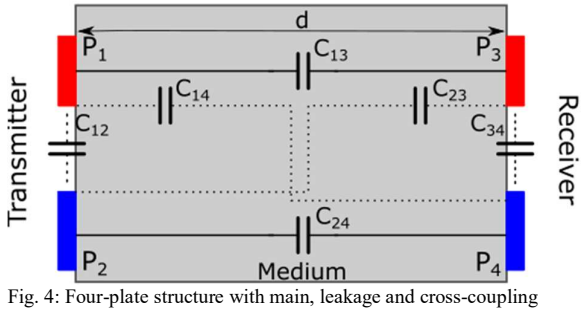

Fig. 4: Four-plate structure with main, leakage and cross-coupling

The size of these capacitances, especially the main capacitance, is determined by the surface of the plates (A), the distance between the plates (d) and the dielectric constant of the medium or relative permittivity (ε_r). The main capacitance can be calculated as follows:

$$C = \varepsilon_r \frac{A}{d} \tag{1}$$

The parasitic capacitances (C_{12}, C_{14}, C_{23}, C_{34}) are impractical to determine by analytical calculations. Therefore, the parasitic capacitances can either be neglected in analytical calculations or determined by means of finite-element simulations. These simulations use a Pi-model as in Fig. 5. This schematic is easier to handle than the one in Fig. 4 [5], [6]. The primary (C_P), secondary (C_S) and mutual (C_M) capacitance then can be calculated as [1], [5], [6]:

$$C_P = \frac{(C_{13} + C_{14}) \cdot (C_{23} + C_{24})}{C_{13} + C_{14} + C_{23} + C_{24}} \tag{2}$$

$$C_S = \frac{(C_{13} + C_{23}) \cdot (C_{14} + C_{24})}{C_{13} + C_{14} + C_{23} + C_{24}} \tag{3}$$

$$C_M = \frac{(C_{13} \cdot C_{24}) - (C_{14} + C_{23})}{C_{13} + C_{14} + C_{23} + C_{24}} \tag{4}$$

In the literature, CPT is often presented with air as the only medium between plates [7]–[9]. This is presumably because CPT has been seen as an alternative to IPT, which already has many application areas where air serves as the medium. However, if another medium increases the energy transfer in CPT, this could open up new application areas where IPT is less viable [10].

Previous studies have shown that the electrical power that can be transferred depends on the size of the coupling capacitance. In theory, the greater the coupling capacitance, the greater the power that can be transmitted [2], [8]. Considering Eqn. (1), the total capacitance can be increased by selecting a medium with a large dielectric constant. For this reason, media such as water, insulation material, glass or concrete allow for greater electrical power to be transferred than air as their dielectric constants are 3 to 80 times greater [11]–[16].

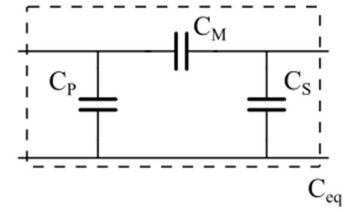

Fig. 5: Pi-model for the capacitive coupling.

III. Theoretical Analysis

The capacitances C_{13} & C_{24} of the plate structure in Fig. 4 perform the power transfer. These capacitances are calculated taking the geometry and medium into account using Eqn. (1). First, parasitic capacities are neglected here and the capacitive coupling factor k_e is assumed to be one. This means that the primary (C_P), secondary (C_S) and mutual (C_M) capacity in the Pi-model of Fig. 5 equal half the main capacitance [1], [2], [6]. In this paper, the mutual capacitance C_M is used to compare different mediums as a larger C_M means higher power transfer [8].

The analytical calculations were carried out for a square plate with a side of 30 cm, altering the distance from 1 mm to 20 cm. Fig. 6 shows the resulting capacitance C_M for six different materials in the gap. The materials used in this analytical comparison are listed in Table 1 with their dielectric constants.

Table 1: Materials with dielectric constants

Material	Dielectric constant
Air	1.0058986 [11]
Brick	3.3 [12]
Rockwool	4.7 [13]
Concrete	4.96 [14]
Glass	7.6 [15]
Water	80.103 [16]

A first finding here is that the resulting C_M with water as a medium is much higher, 80 times according to dielectric

constant, than in air. Even typical building materials like glass or rockwool lead to a significantly higher resulting capacitance, 3 to 8 times greater at a distance of 10 mm. In the next section, we will extend the investigation with parasitic capacitances using finite-element simulation.

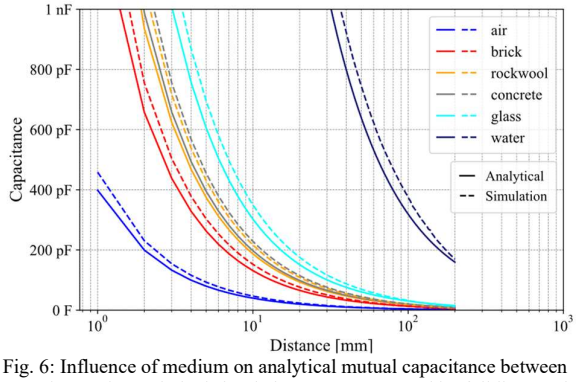

Fig. 6: Influence of medium on analytical mutual capacitance between two plates. The analytical simulations are represented by full lines and finite-elements simulations by dashed lines.

IV. Simulation Results

A. Coupling capacitance

To model the leakage and cross-coupling capacitances, a finite-element simulation software such as CST Studio Suite is required. The simulation model, as in Fig. 7, is based on the same parameters of the analytical calculations in Fig. 4. The model output is a symmetric capacitance matrix:

$$C_{coupler} = \begin{bmatrix} C_{11} & C_{12} & C_{13} & C_{14} \\ C_{21} & C_{22} & C_{23} & C_{24} \\ C_{31} & C_{32} & C_{33} & C_{34} \\ C_{41} & C_{42} & C_{43} & C_{44} \end{bmatrix} \quad (5)$$

The self-capacitances of the plates (C_{11}, C_{22}, C_{33}, C_{44}) are listed at the diagonal of the matrix $C_{coupler}$ in Eqn. (5). These are neglected in this paper because the distance between the plates is much smaller than the distance between the plates and their reference at infinity [17]. Additionally, the fringing fields, the electrical conductivity of the medium, the equivalent series resistance and the equivalent series inductance of the capacitive coupling are not taken into account in these finite-element simulations.

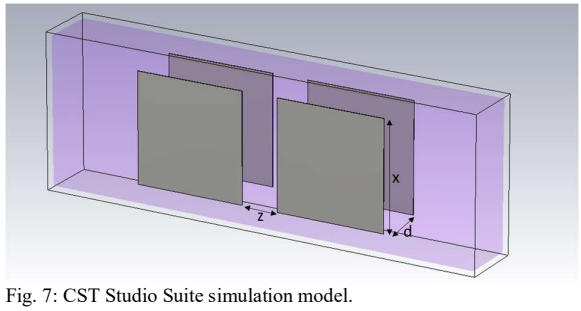

Fig. 7: CST Studio Suite simulation model.

For the described CPT system, the resulting mutual capacitances C_M are presented in Fig. 6 by dashed lines. These simulations included the leakage and cross-coupling capacitances. For plate distances up to 25 mm, the simulation results are about 15 % higher than the analytical calculations. This can be explained by the maximum accuracy of the simulation program of one picofarad. After 25 mm, the capacitances of the finite-elements become smaller than those of the analytical calculations. This is due to the influence of the leakage and cross-coupling capacitance, which can be found in the values of the capacitive coupling coefficient in Fig. 8. Due to the maximum accuracy of the simulation program, the coupling coefficient around a distance of 25 mm, is slightly higher than one.

The capacitive coupling coefficient of water drops faster than the coefficient of air. The advantage of the high permittivity, becomes a disadvantage: cross-coupling and leakage capacities increase and causing the coupling coefficient to drop faster. This reduces the output voltage at the secondary side and deteriorates efficiency of the system [2],[6]. In the next section we will employ the calculated coupling capacitances in an electrical circuit simulation to quantify their effect on the transferrable electrical power.

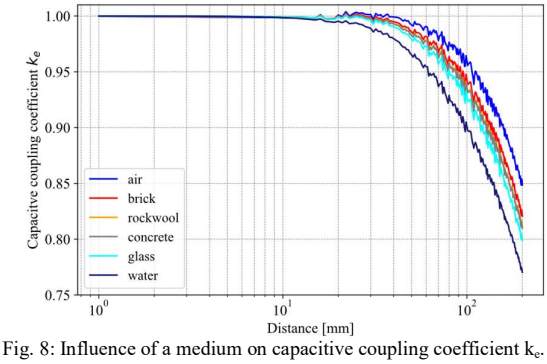

Fig. 8: Influence of a medium on capacitive coupling coefficient k_e.

B. Power electronic simulations

We simulate the power electronic circuit in PLECS to determine the maximum power transfer as a function of the plate distances for different media. The simulated circuit is shown in Fig. 9. A resonator circuit is used with one inductor in series with the coupling capacitors, the latter model the capacitive coupling. The added coil creates series resonance with the primary capacitance C_P, which creates a higher voltages on the plates and also lowers the resonance frequency. The resonant tank reaches a gain of one when the system is operating at the resonance frequency [18]. In order to achieve maximum power transfer for each simulation, the resonance frequency for each distance is calculated according to Eqn. (6), where L_P is the primary inductor and C_{eq} is the equivalent capacitance of the system.

$$f_{res} = \frac{1}{2\pi\sqrt{L_P \cdot C_{eq}}} \quad (6)$$

Table 2: Overview of candidate switching components for CPT and switching limits. [23], [24]

Product	Technology	Breakdown Voltage [V]	Maximum current [A]	Maximum switching frequency based on turn on/off times[MHz]	Maximum switching frequency based on thermal limits [MHz]
UF3C065080K4S	SiC	650	31	11.6	0.94
IPT60R090CFD7	SiC	600	28	7.5	0.55
GS66508T	GaN	650	30	47.6	0.57
GAN063-650WSA	GaN	650	31	6.0	1.53
TP65H050WS	GaN	650	36	6.3	1.02

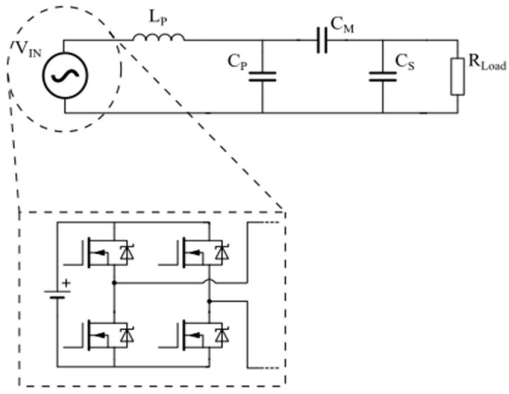

Fig. 9: PLECS simulation model.

The resonance frequency increases as the capacitance of the system decreases when the distance between the plates increases. In theory, very large transfer distances can be achieved with a frequency towards infinity. In practice, power electronic switches are a limiting factor. They contain two limits: on the one hand, the maximum achievable switching frequency, which is determined by the internal capacitances of the switching component and its switching behaviour in general . On the other hand, there is a thermal limit due to conduction losses (P_{cond}) and the increasing switching losses at higher switching frequencies (P_{sw}). In this paper, those losses are based following formulas [19], [20]:

$$P_{cond} = \frac{1}{2} \cdot R_{ds,on} \cdot I_{in}^2 \tag{7}$$

$$P_{sw} = \frac{1}{2} \cdot V_{in} \cdot I_{in} \cdot (t_{rise} + t_{fall}) \cdot f_{sw} \tag{8}$$

Table 2 shows five typical power electronic switches with crucial parameters. The maximum switching frequency is mainly determined by the thermal limit. This was determined by taking into account the conduction and switching losses for a square wave PWM. The switching losses increase linearly with the switching frequency and become the most important component at high frequencies. The total losses per switching component in a system with a thermal interface pad and heat sink result in a temperature rise. To ensure a long service life of the component, the maximum temperature rise is limited to 50 K. This results in Fig. 10.

From calculations and literature it can be concluded that power electronic switches with GaN-technology are most suitable for CPT systems as they are able to switch at frequencies higher than 1 MHz [21]–[24]. For this reason, the maximum system frequency is limited to 1 MHz in this paper.

The electrical parameters of the simulation were determined on the one hand by the limitations of the switching components and, on the other hand by the connected grid. An ideal inverter generates an AC signal with an amplitude of 400 V at the desired frequency feeding the plates. This inverter is represented in the simulation as an ideal controllable voltage source. The output voltage of the inverter will be kept constant while the frequency will be tuned to the resonance frequency of the system. The load is a 500 Ω resistor, that has arbitrarily chosen. The simulations were performed with the parameters from

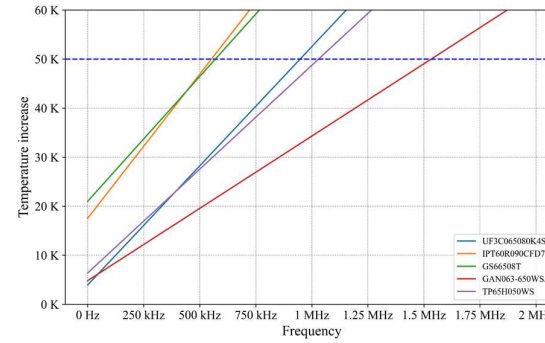

Fig. 10: Temperature increase of switching components because of

Table 3, resulting in output power as a function of the plate distance in Fig. 11. It shows that for a given setting, glass allows CPT to transfer 1 kW over 3 to 4 mm while in air such a power transfer is not even possible at 1 mm.

Table 3: Simulation parameters

Parameter	Value
V_{in}	400 V
L_P	200 µH
R_{Load}	500 Ω

According to these simulations, the medium affects the resonant frequency and thus the resulting power output. Media with a high dielectric constant allow higher powers to be transmitted over a greater distance. This is demonstrated by water and glass in Fig. 11. CPT in water and glass each reach a maximum power output of approximately 2 kW while the maximum power output in air is only 500 W. The maximum power transmission in water and glass is achieved at 11 mm and 1 mm respectively. For water as a medium, the peak of power transfer is the moment at which the impedance of the coil in combination with capacitive coupling is equal to the load. This results in the lowest system impedance and the highest possible power transfer in this system.

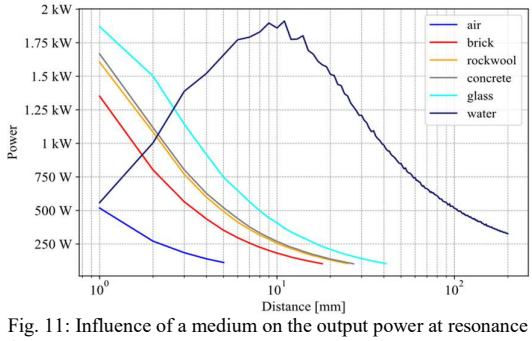

Fig. 11: Influence of a medium on the output power at resonance frequency.

Water achieves significantly greater transfer distances and power than the other media. These results can be explained by the relative permittivity which is 11 to 80 times greater than that of the other simulated materials. An additional benefit of having a lower resonant frequency is that switching losses will be reduced. The resonant frequency for the system in water was throughout all simulations 9 to 12 times smaller than in air.

CONCLUSION

The finite-element simulations have shown that as the distance between the plates increases, the parasitic capacitances become more important. The greater the relative permittivity of the material, the greater the influence of the parasitic capacity. This is confirmed by the decreasing behaviour of the capacitive coupling coefficient in function of the distance between the plates.

Based on the finite-element simulations, the capacitive coupling of capacitive power transfer system with single resonator was simulated. The simulations demonstrated that a medium with a high dielectric constant can ensure higher transmit power over greater distances at lower frequencies. For example, in these simulations glass allows CPT to transfer 1 kW over 3 to 4 mm while in air only 500 W can be reached at 1 mm.

In the future, this will be extended and will take into account fringing fields, electrical conductivity of the medium, the equivalent series resistance and the equivalent series inductance of the capacitive coupling. Furthermore, a more detailed modelling of the power converter topology is needed and possible applications must be identified and simulated. Finally, findings from simulations will be validated with a laboratory setup.

REFERENCES

[1] C. Lecluyse, B. Minnaert, and M. Kleemann, “A Review of the Current State of Technology of Capacitive Wireless Power Transfer,” Energies, vol. 14, no. 18, p. 5862, Sep. 2021.

[2] F. Lu, H. Zhang, and C. Mi, “A Review on the Recent Development of Capacitive Wireless Power Transfer Technology,” Energies, vol. 10, no. 11, p. 1752, Nov. 2017.

[3] B. Minnaert and N. Stevens, “Optimal Analytical Solution for a Capacitive Wireless Power Transfer System with One Transmitter and Two Receivers,”Energies, vol. 10, no. 9, p. 1444, Sep. 2017.

[4] J. Dai and D. C. Ludois, “A Survey of Wireless Power Transfer and a Critical Comparison of Inductive and Capacitive Coupling for Small Gap Applications,” IEEE Transactions on Power Electronics, vol. 30, no. 11, pp. 6017–6029, 2015, doi: 10.1109/TPEL.2015.2415253.

[5] C. Liu, A. P. Hu, and M. Budhia, “A generalized coupling model for Capacitive Power Transfer systems,” IECON Proceedings (Industrial Electronics Conference), pp. 274–279, 2010, doi: 10.1109/IECON.2010.5675014.

[6] L. Huang and A. P. Hu, “Defining the mutual coupling of capacitive power transfer for wireless power transfer,” Electronics Letters, vol. 51, no. 22, pp. 1806–1807, 2015, doi: 10.1049/el.2015.2709.

[7] A. Kumar, S. Pervaiz, C. K. Chang, S. Korhummel, Z. Popovic, and K. K. Afridi, “Investigation of power transfer density enhancement in large air-gap capacitive wireless power transfer systems,” 2015 IEEE Wireless Power Transfer Conference, WPTC 2015, 2015, doi: 10.1109/WPT.2015.7140182.

[8] H. Zhang, F. Lu, H. Hofmann, W. Liu, and C. C. Mi, “Six-Plate Capacitive Coupler to Reduce Electric Field Emission in Large Air-Gap Capacitive Power Transfer,” IEEE Transactions on Power Electronics, vol. 33, no. 1, pp. 665–675, 2018, doi: 10.1109/TPEL.2017.2662583.

[9] H. Zhang, F. Lu, H. Hofmann, W. Liu, and C. Mi, “A large air-gap capacitive power transfer system with a 4-plate capacitive coupler structure for electric vehicle charging applications,” Conference Proceedings - IEEE Applied Power Electronics Conference and Exposition - APEC, vol. 2016-May, pp. 1726–1730, 2016, doi: 10.1109/APEC.2016.7468100.

[7] [10] A. Kumar, S. Pervaiz, C. K. Chang, S. Korhummel, Z. Popovic, and K. K. Afridi, “Investigation of power transfer density enhancement in large air-gap capacitive wireless power transfer systems,” 2015 IEEE Wireless Power Transfer Conference, WPTC 2015, 2015, doi: 10.1109/WPT.2015.7140182.

[8] H. Zhang, F. Lu, H. Hofmann, W. Liu, and C. C. Mi, “Six-Plate Capacitive Coupler to Reduce Electric Field Emission in Large Air-Gap Capacitive Power Transfer,” IEEE Transactions on Power Electronics, vol. 33, no. 1, pp. 665–675, 2018, doi: 10.1109/TPEL.2017.2662583.

[9] H. Zhang, F. Lu, H. Hofmann, W. Liu, and C. Mi, “A large air-gap capacitive power transfer system with a 4-plate capacitive coupler structure for electric vehicle charging applications,” Conference Proceedings - IEEE Applied Power Electronics Conference and Exposition - APEC, vol. 2016-May, pp. 1726–1730, 2016, doi: 10.1109/APEC.2016.7468100.

[10] B. Minnaert, S. Ravyts, J. Driesen and N. Stevens, "Challenges for Wireless Power Transfer in Building-Integrated Photovoltaics," 2018 IEEE PELS Workshop on Emerging Technologies: Wireless Power Transfer (Wow), 2018, pp. 1-5, doi: 10.1109/WoW.2018.8450923.

[11] L. G. Hector and H. L. Schultz, “The dielectric constant of air at radiofrequencies,” Journal of Applied Physics, vol. 7, no. 4, pp. 133–136, 1936, doi: 10.1063/1.1745374.

[12] A. Choroszucho, B. Butrylo, A. Steckiewicz, and J. M. Stankiewicz, “Determination of the Effective Electromagnetic Parameters of Complex Building Materials for Numerical Analysis of Wireless Transmission Networks,” Electronics, vol. 9, no. 10, p. 1569, Sep. 2020, doi: 10.3390/electronics9101569.

[13] O. M. Nofal and A. M. Zihlif, “Dielectric and AC conductivity of rockwool fibers-polystyrene composites,” Journal of Reinforced Plastics and Composites, vol. 29, no. 17, pp. 2636–2646, 2010, doi: 10.1177/0731684409357258.

[14] H. Xu, B. Li, S. Xu, and H. Feng, “The measurement of dielectric constant of the concrete using single-frequency CW radar,” Proceedings - The 1st International Conference on Intelligent Networks and Intelligent Systems, ICINIS 2008, pp. 588–591, 2008, doi: 10.1109/ICINIS.2008.139.

[15] ACG, “Technical Data Sheet – Thermobel,” Feb. 2012.

[16] C. G. Malmberg and A. A. Maryott, “Dielectric constant of water from 0 to 100 C,” Journal of Research of the National Bureau of Standards, vol. 56, no. 1, p. 1, 1956, doi: 10.6028/jres.056.001.

[17] Q. Zhu, S. Zang, L. J. Zou, G. Zhang, M. Su, and A. P. Hu, “Study of coupling configurations of capacitive power transfer system with four metal plates,” Wireless Power Transfer, pp. 97–112, 2019, doi: 10.1017/wpt.2019.10.

[18] D. Rozario, N. A. Azeez and S. S. Williamson, "Comprehensive review and comparative analysis of compensation networks for Capacitive Power Transfer systems," 2016 IEEE 25th International Symposium on Industrial Electronics (ISIE), 2016, pp. 823-829, doi: 10.1109/ISIE.2016.7744996.

[19] A. Lidow, J. Strydom, M. de Rooij, and D. Reusch, GaN Transistors for Efficient Power Conversion. John Wiley & Sons, 2015.

[20] N. Mohan, T. Undeland, and W. Robbins, Power Electronics: Converters, Applications, Third. John Wiley & Sons, 2003.

[21] K. Gopalakrishna, "Frequency Characterization of Si, SiC, and GaN MOSFETs Using Frequency Characterization of Si, SiC, and GaN MOSFETs Using Buck Converter In CCM as an Application Buck Converter In CCM as an Application," M.S. thesis, Department of Electrical Engineering, Wright State University, Dayton, Ohio, 2013. Accessed on Apr. 04, 2022. [Online]. Available: https://corescholar.libraries.wright.edu/etd_allhttps://corescholar.libraries.wright.edu/etd_all/1343

[22] C.-T. Ma and Z.-H. Gu, "Review on Driving Circuits for Wide-Bandgap Semiconductor Switching Devices for Mid- to High-Power Applications," Micromachines, vol. 12, no. 1, p. 65, Jan. 2021, doi: 10.3390/mi12010065.

[23] Mouser, "MOSFET." https://www.mouser.be/ (accessed Apr. 04, 2022).

[24] Digikey, "Transistors - FETs, MOSFETs - Single." https://www.digikey.be/en (accessed Apr. 04, 2022).